Recent results from the GlueX collaboration

Yannick Wunderlich

HISKP, University of Bonn

September 20th, 2024

Plan for the talk

I.) Introduction

II.) The GlueX experiment

III.) 2-meson photoproduction and extraction of spin-density matrix elements (SDMEs)

IV.) Results from GlueX:

- SDMEs for $\rho(770)$ and $\Delta^{++}(1232)$ photoproduction
- $a_2(1260)$-photoproduction at GlueX
- Upper limits for production of the $\pi_1(1600)$

Introduction & motivation

The spectrum of hadrons is generated by the $SU(3)_c$ gauge-theory of QCD

*) Standard quark-model classification:
$|\mathrm{meson}\rangle = |q\bar{q}\rangle$, $|\mathrm{baryon}\rangle = |qqq\rangle$;
$\hookrightarrow$ many found; consistent with QCD

*) However: multiquark-configurations $\left(|q\bar{q}q\bar{q}\rangle , |qqqq\bar{q}\rangle , \ldots \right)$ are in principle allowed as well

*) Nonlinear QFT-dynamics (!)
$\Rightarrow$ hybrid configurations $|q\bar{q}g\rangle$ allowed as well, ...
$\Rightarrow$ ... as are glueballs $|gg\rangle$.

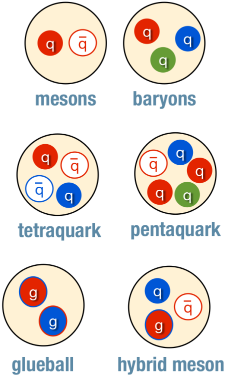

Introduction & motivation

The spectrum of hadrons is generated by the $SU(3)_c$ gauge-theory of QCD

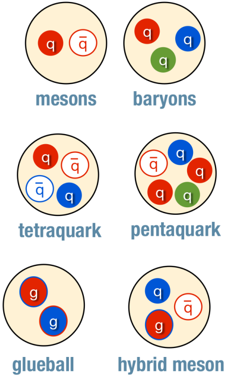

∗) Standard quark-model classification:
$|\text{meson}\rangle = |q\bar{q}\rangle$, $|\text{baryon}\rangle = |qqq\rangle$;
↪ many found; consistent with QCD

∗) However: multiquark-configurations $\left(|q\bar{q}q\bar{q}\rangle \right.$, $\left. |qqqq\bar{q}\rangle, \ldots \right)$ are in principle allowed as well

∗) Nonlinear QFT-dynamics (!)
⇒ hybrid configurations $|q\bar{q}g\rangle$ allowed as well, ...
⇒ ... as are glueballs $|gg\rangle$.

∗) In standard quark-model, one has, for a $|q\bar{q}\rangle$-state:
$\vec{J} = \vec{L} \oplus \vec{S}$, $\boldsymbol{P}(q\bar{q}) = (-1)^{L+1}$ and $\boldsymbol{C}(q\bar{q}) = (-1)^{L+S}$.

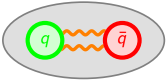

⇒ Allowed: $J^{PC} = 0^{-+}, 0^{++}, 1^{--}, 1^{+-}, \ldots$; Forbidden: $J^{PC} = 0^{--}, 0^{+-}, 1^{-+}, 2^{+-}, \ldots$

∗) Spin-exotic quantum numbers are "smoking gun" for states inconsistent with a pure $|q\bar{q}\rangle$-system ↪ GlueX: hybrid searches ...

Hybrid mesons from Lattic QCD

Excited spectrum of isoscalar mesons using lattice QCD (hadspec collaboration):

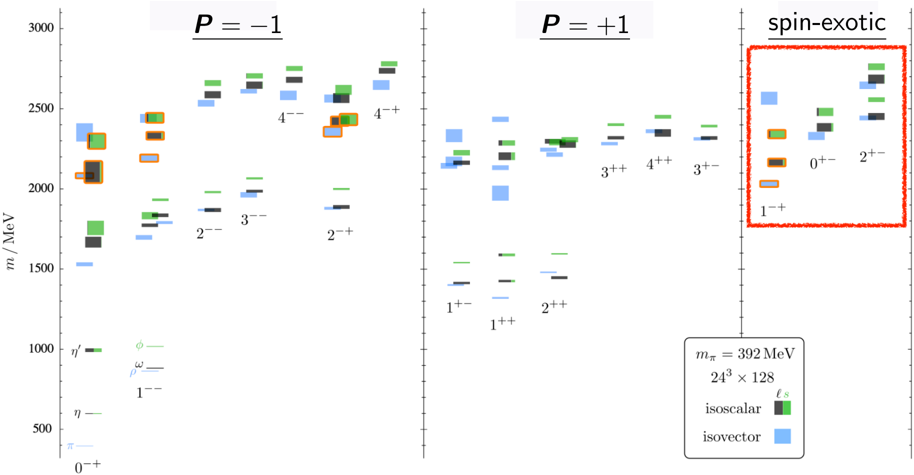

[J. J. Dudek *et al.* [Hadron Spectrum], Phys. Rev. D **88**, no.9, 094505 (2013)]

CEBAF facility at Jefferson Lab

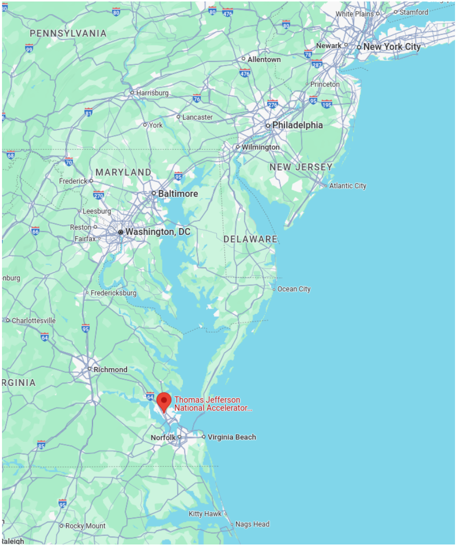

The GlueX experiment (Hall D)

Linearly polarized photon-beam ($P \simeq 40$ %) via coherent bremsstrahlung on a thin diamond:

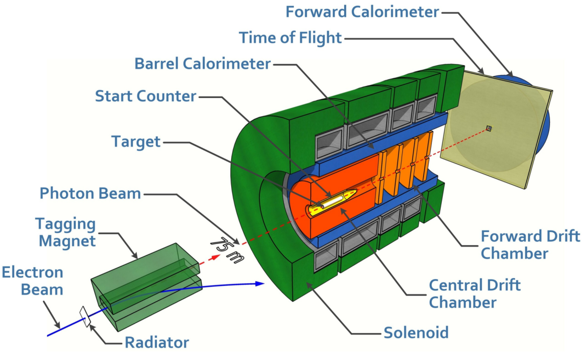

Almost complete phase-space coverage for measurements of neutral and charged particles:

- ∗) Acceptance: $\theta^{\mathrm{LAB}} \in [1, \ldots, 120]^{\circ}$
- ∗) Charged particles: $\frac{\sigma_p}{p} \simeq 1, \ldots, 3\%$

Determine photon-energy via tagged recoil-electrons:

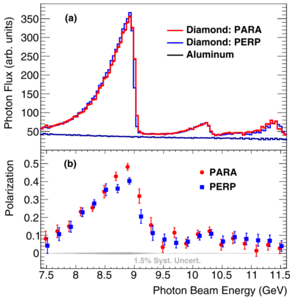

[Nucl. Inst. Meth. A, **987**, 164807 (2021)]

Phases of GlueX:

Phase	$\int \mathcal{L}$ [pb^{-1}]
GlueX-I (2017-2018)	330 ($E_\gamma > 8$ GeV)
GlueX-II (2020-2025)	$\simeq$ 320 (so far ...)
GlueX-III (?)	$\simeq$ 800

Merits of (2-meson) photoproduction

Photoproduction is a useful tool, because:

- ∗) Diffractive production well-understood (exchange mechanisms)
- ∗) Photoproduction yields complementary information to pion-induced data (e.g. COMPASS)
- ∗) Current world photoproduction-data scarce at GlueX-energies
- ∗) Use polarization to constrain production mechanisms

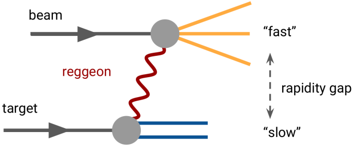

[J. Nys *et al.* [JPAC], PRD **98**, 3, 034020 (2018)]

Merits of (2-meson) photoproduction

Photoproduction is a useful tool, because:

- $*$) Diffractive production well-understood (exchange mechanisms)

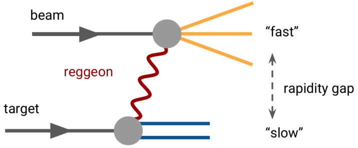

[J. Nys *et al.* [JPAC], PRD **98**, 3, 034020 (2018)]

- $*$) Photoproduction yields complementary information to pion-induced data (e.g. COMPASS)
- $*$) Current world photoproduction-data scarce at GlueX-energies
- $*$) Use polarization to constrain production mechanisms
- $*$) Can produce a large variety of quantum numbers:

'Reggeon'		Exotic final states	
$\mathbb{P}$	0^{++}	b, h, h'	2^{+-}, 0^{+-}
π^0	0^{-+}	b_2, h_2, h_2'	2^{+-}
$\pi^\pm$	0^{-+}	$\pi_1^\pm$	1^{-+}
ω	1^{--}	π_1, η_1, η_1'	1^{-+}

Merits of (2-meson) photoproduction

Photoproduction is a useful tool, because:

- ∗) Diffractive production well-understood (exchange mechanisms)
- ∗) Photoproduction yields complementary information to pion-induced data (e.g. COMPASS)
- ∗) Current world photoproduction-data scarce at GlueX-energies
- ∗) Use polarization to constrain production mechanisms
- ∗) Can produce a large variety of quantum numbers:

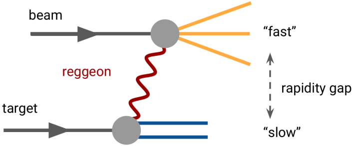

[J. Nys *et al.* [JPAC], PRD **98**, 3, 034020 (2018)]

'Reggeon'		Exotic final states	
$\mathbb{P}$	0^{++}	b, h, h'	2^{+-}, 0^{+-}
π^0	0^{-+}	b_2, h_2, h_2'	2^{+-}
$\pi^\pm$	0^{-+}	$\pi_1^\pm$	1^{-+}
ω	1^{--}	π_1, η_1, η_1'	1^{-+}

Focus on decays to $\eta\pi$ and $\eta'\pi$ ('golden channels')
$\Rightarrow$ 'flagship reactions' involving recoil against either a proton or a Δ-isobar
(e.g. $\gamma p \longrightarrow \eta\pi^0 p, \ldots$)

Extraction of spin-density matrix elements (SDMEs)

Assume: Only one 2-body subsystem, with certain spin, is known to propagate (e.g. due to cuts applied to data), i.e.:

[Figs: V. Mathieu, Talk, NSTAR2024]

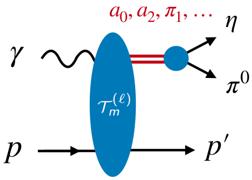

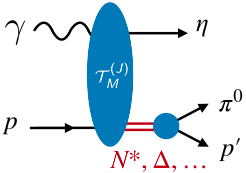

Extraction of spin-density matrix elements (SDMEs)

Assume: Only one 2-body subsystem, with certain spin, is known to propagate (e.g. due to cuts applied to data), i.e.:

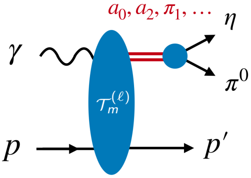

[Figs: V. Mathieu, Talk, NSTAR2024]

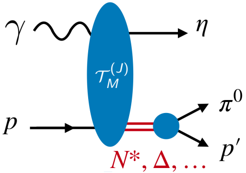

⇒ This fixes angular dependence of the intensity (cf. helicity-formalism, tensor-formalism, ...), e.g. for ρ-meson photoproduction (for polarized $\vec{\gamma}$):

$$I(\Omega, \Phi) = I^0(\Omega) - P_\gamma \cos(2\Phi) I^1(\Omega) - P_\gamma \sin(2\Phi) I^2(\Omega),$$

$$I^0(\Omega) = \frac{3}{4\pi}\left[\frac{1}{2}\left(1-\rho^0_{00}\right) + \frac{1}{2}\left(3\rho^0_{00}-1\right)\cos^2\theta - \sqrt{2}\mathrm{Re}\rho^0_{10}\sin 2\theta\cos\phi - \rho^0_{1,-1}\sin^2\theta\cos 2\phi\right],$$

$$I^1(\Omega) = \frac{3}{4\pi}\left[\rho^1_{11}\sin^2\theta + \rho^1_{00}\cos^2\theta - \sqrt{2}\mathrm{Re}\rho^1_{10}\sin 2\theta\cos\phi - \rho^1_{1,-1}\sin^2\theta\cos 2\phi\right],$$

$$I^2(\Omega) = \frac{3}{4\pi}\left[\sqrt{2}\mathrm{Im}\rho^2_{10}\sin 2\theta\sin\phi + \mathrm{Im}\rho^2_{1,-1}\sin^2\theta\sin 2\phi\right].$$

Extraction of spin-density matrix elements (SDMEs)

Assume: Only one 2-body subsystem, with certain spin, is known to propagate (e.g. due to cuts applied to data), i.e.:

[Figs: V. Mathieu, Talk, NSTAR2024]

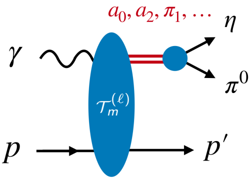

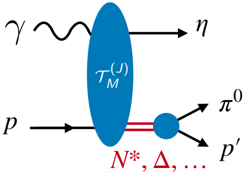

$\Rightarrow$ This fixes angular dependence of the intensity (cf. helicity-formalism, tensor-formalism, ...), e.g. for ρ-meson photoproduction (for polarized $\vec{\gamma}$):

$$I(\Omega, \Phi) = I^0(\Omega) - P_\gamma \cos(2\Phi) I^1(\Omega) - P_\gamma \sin(2\Phi) I^2(\Omega),$$

$$I^0(\Omega) = \frac{3}{4\pi}\left[\frac{1}{2}\left(1 - \rho^0_{00}\right) + \frac{1}{2}\left(3\rho^0_{00} - 1\right)\cos^2\theta - \sqrt{2}\mathrm{Re}\rho^0_{10}\sin 2\theta\cos\phi - \rho^0_{1,-1}\sin^2\theta\cos 2\phi\right],$$

$$I^1(\Omega) = \frac{3}{4\pi}\left[\rho^1_{11}\sin^2\theta + \rho^1_{00}\cos^2\theta - \sqrt{2}\mathrm{Re}\rho^1_{10}\sin 2\theta\cos\phi - \rho^1_{1,-1}\sin^2\theta\cos 2\phi\right],$$

$$I^2(\Omega) = \frac{3}{4\pi}\left[\sqrt{2}\mathrm{Im}\rho^2_{10}\sin 2\theta\sin\phi + \mathrm{Im}\rho^2_{1,-1}\sin^2\theta\sin 2\phi\right].$$

$\Rightarrow$ Fit SDMEs ρ^i_{jk} out of the data and compare to models;

SDMEs are bilinear: $\rho^0_{m,m'} = \mathcal{T}_m^{(\ell)}\mathcal{T}_{m'}^{(\ell)*}, \ldots$

Example I: SDMEs for $\rho(770)$-production

- Reaction:
  $$\vec{\gamma} p \longrightarrow \underbrace{\rho(770)}_{\to \pi^+ \pi^-} p$$
- SDMEs are orders of magnitude more precise than previous measurements, with only a fraction of the full GlueX dataset,
- Uncertainties are dominated by systematics,
- Agreement with Regge-model [JPAC, PRD **97**, 094003 (2018)] is good up to $-t \simeq 0.5 \mathrm{GeV}^2/c^2$
- In progress: ϕ, ω

[GlueX, Phys. Rev. C **108**, 5, 055204 (2023)]

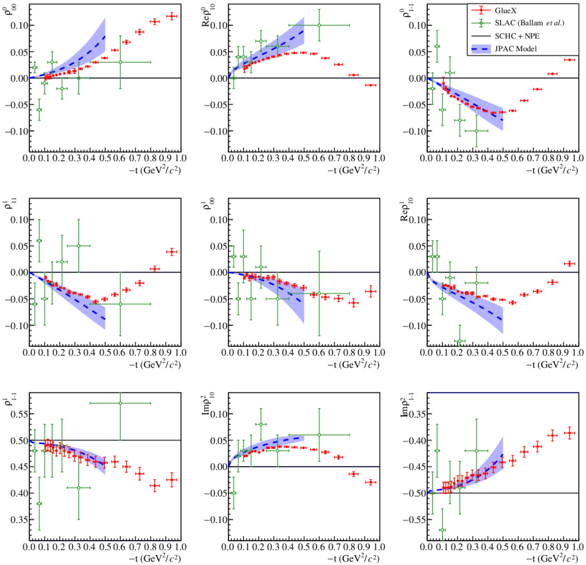

Example II: SDMEs for $\Delta^{++}(1232)$-production

∗) Reaction:

$$\vec{\gamma} p \rightarrow \pi^{-} \underbrace{\Delta^{++}(1232)}_{\rightarrow \pi^{+} p}$$

∗) Statistics superior to previously measured data (SLAC),

∗) Data useful for constraining bottom vertex of the reaction

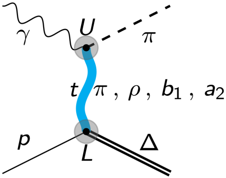

[Fig.: V. Shastry]

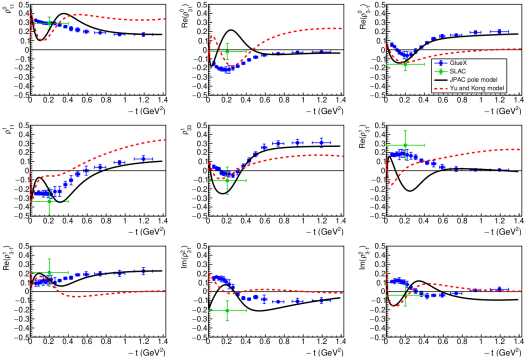

[F. Afzal *et al.* [GlueX], arXiv:2406.12829 [nucl-ex]]

Example II: SDMEs for $\Delta^{++}(1232)$-production

∗) Reaction:

$$\vec{\gamma} p \rightarrow \pi^- \underbrace{\Delta^{++}(1232)}_{\rightarrow \pi^+ p}$$

∗) Statistics superior to previously measured data (SLAC),

∗) Data useful for constraining bottom vertex of the reaction

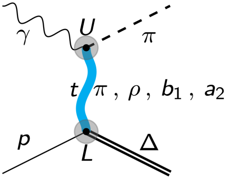

[Fig.: V. Shastry]

∗) Natural-parity exchange described well by JPAC model

[JPAC, PLB **779**, 77 (2018)]

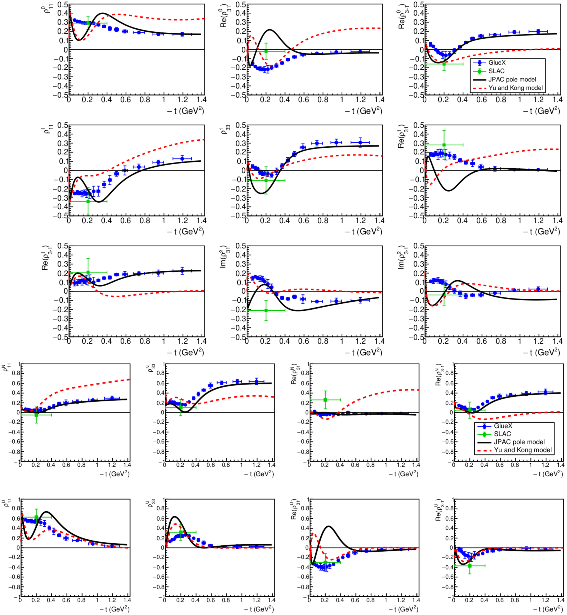

[F. Afzal *et al.* [GlueX], arXiv:2406.12829 [nucl-ex]]

$a_2(1320)$-photoproduction - I

$*)$ Strong evidence for spin-exotic $\pi_1(1600)$-contribution from COMPASS;
$\Rightarrow$ Key GlueX-channel to compare to: $\gamma p \longrightarrow \pi\eta N$,

$*)$ Clear signals seen in the data, at $a_0(980)$- and $a_2(1320)$-masses,

$0.1 < -t < 0.3$ GeV^2

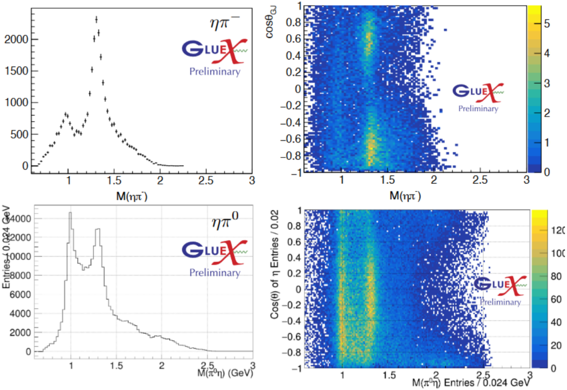

$a_2(1320)$-photoproduction - I

$*$) Strong evidence for spin-exotic $\pi_1(1600)$-contribution from COMPASS;
$\Rightarrow$ Key GlueX-channel to compare to: $\gamma p \longrightarrow \pi \eta N$,

$*$) Clear signals seen in the data, at $a_0(980)$- and $a_2(1320)$-masses,

$0.1 < -t < 0.3$ GeV^2

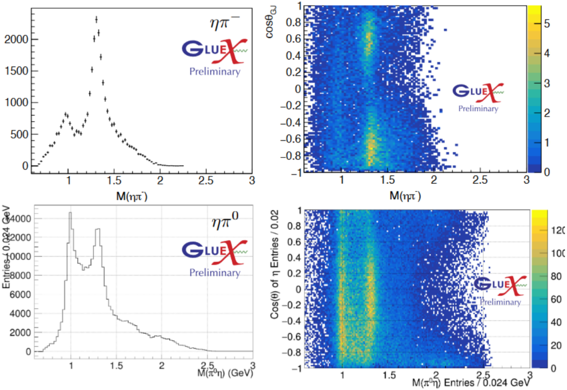

$*$) Angular dist. of the $a_2(1320)$-signal different between charged- and neutral channels,
$\hookrightarrow$ Different spin-m projections populated,

$*$) Need amplitude analysis for strong $a_2(1320)$-signal, as 'reference-wave' for interference off (smaller) π_1-signal,

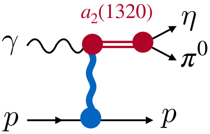

[Fig: V. Mathieu]

$a_2(1320)$-photoproduction - II

Semi mass-dependent method: use Breit-Wigner parametrization for the $a_2(1320)$
$\oplus$ mass-independent 'parametrization' for the S-wave amplitudes;
$\hookrightarrow$ Fit performed only with 'coherent' S- and D-waves,

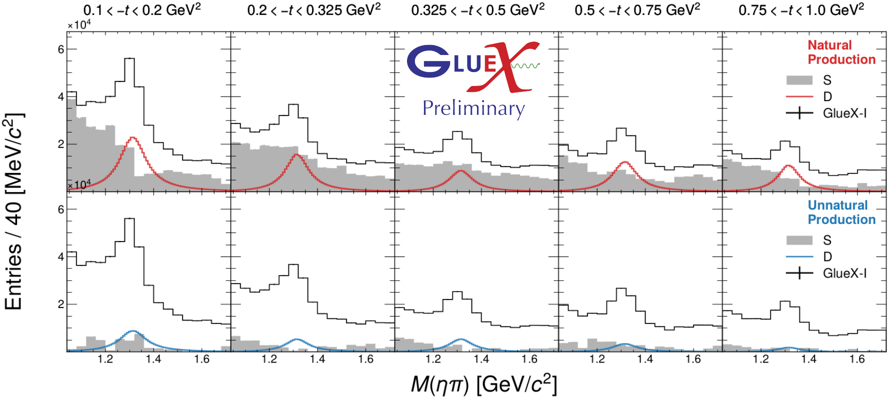

a_2(1320)-photoproduction - III

*) Agreement with JPAC TMD-model [JPAC, PRD **102**, 014003 (2020)] at least reasonable,

*) Dominance of natural parity exchanges $(\rho, \omega, \ldots)$ observed,

*) Statistical errors from bootstrapping;
elaborate systematics studies performed in addition,

⇒ [Publication currently in preparation . . .]

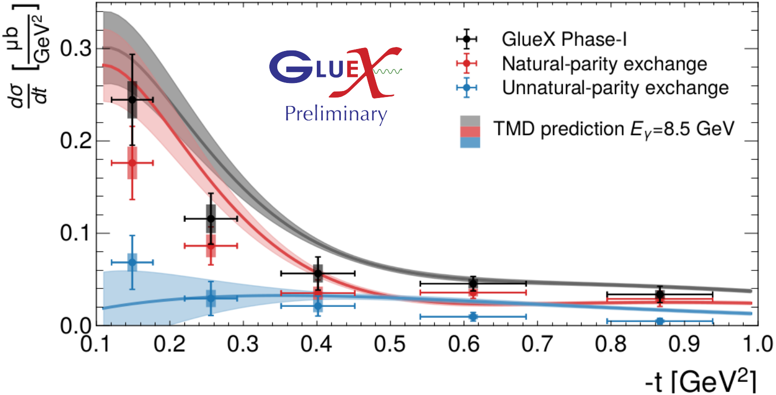

$\pi_1(1600)$ upper limits - I

Use GlueX-measurements for 3 ω-photoproduction reactions:

$$\gamma p \longrightarrow \omega\pi^+\pi^- p,\ \gamma p \longrightarrow \omega\pi^0\pi^0 p \text{ and } \gamma p \longrightarrow \omega\pi^-\pi^0\Delta^{++}.$$

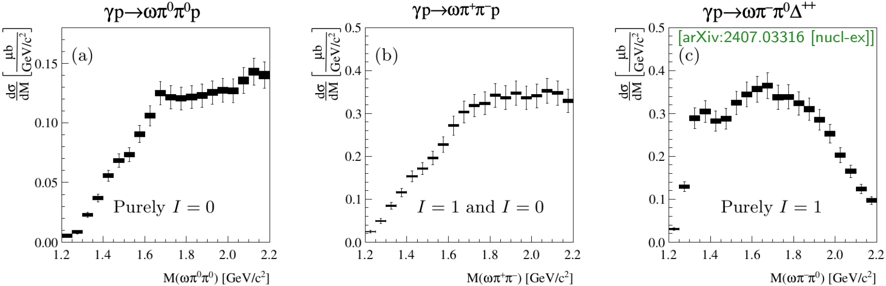

$\pi_1(1600)$ upper limits - I

Use GlueX-measurements for 3 ω-photoproduction reactions:

$\gamma p \longrightarrow \omega\pi^+\pi^- p$, $\gamma p \longrightarrow \omega\pi^0\pi^0 p$ and $\gamma p \longrightarrow \omega\pi^-\pi^0\Delta^{++}$.

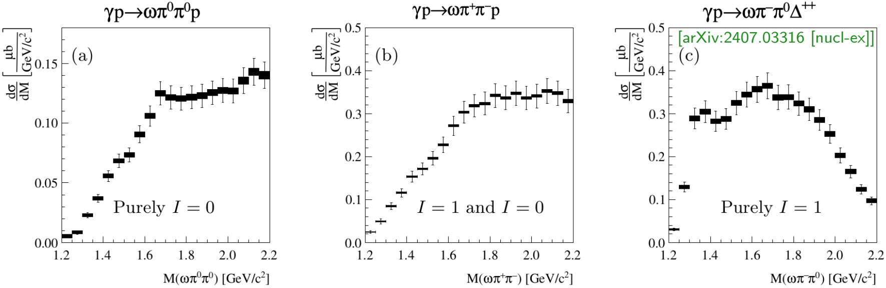

$*$) Upper limit on $\pi(1600)$-production is set using isospin-separation, assuming no $I = 2$:

$$\sigma\left(\omega\pi\pi\right)^{0}_{I=1} = \sigma\left(\omega\pi^{+}\pi^{-}\right) - 2\sigma\left(\omega\pi^{0}\pi^{0}\right),$$

$$\sigma\left(\omega\pi\pi\right)^{-}_{I=1} = \sigma\left(\omega\pi^{-}\pi^{0}\right).$$

$\Rightarrow$ Fit $\sigma\left(\omega\pi\pi\right)_{I=1}$ using known resonance parameters for the $a_2(1320)$ (from PDG) and the $\pi_1(1600)$ (JPAC),

$\pi_1(1600)$ upper limits - II

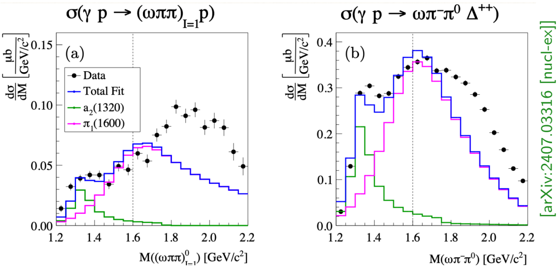

- $*$) Fit-range: $M\left(\omega\pi\pi\right)_{I=1} < 1.6\ \mathrm{GeV}/c^2$
- $*$) Adjust a_2-shape to measured cross section, with known BR,
- $*$) π_1-BR from Lattice QCD,
- $*$) π_1-magnitude is only free parameter (!),

$\Rightarrow$ Upper limits for π_1 roughly similar in size to a_2 cross-sections.

$\pi_1(1600)$ upper limits - II

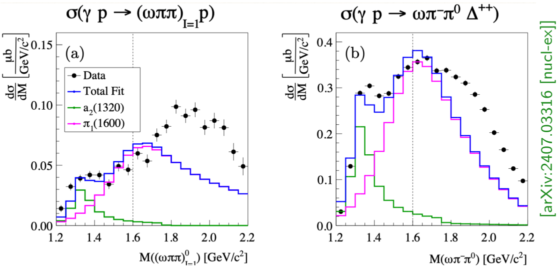

- $*)$ Fit-range: $M\left(\omega\pi\pi\right)_{I=1} < 1.6$ GeV$/c^2$
- $*)$ Adjust a_2-shape to measured cross section, with known BR,
- $*)$ π_1-BR from Lattice QCD,
- $*)$ π_1-magnitude is only free parameter (!),

$\Rightarrow$ Upper limits for π_1 roughly similar in size to a_2 cross-sections.

- $*)$ $\pi_1 \rightarrow \eta\pi$: small,
- $*)$ $\pi_1 \rightarrow \eta'\pi$: dominates the spectrum,

$\Rightarrow$ Important constraints for amplitude analyses, ...

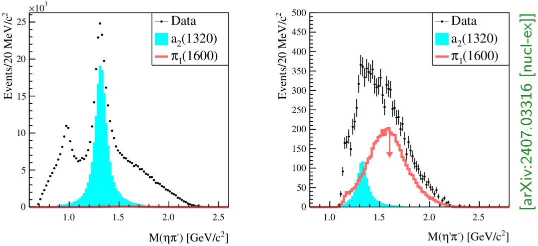

Conclusions & Outlook

∗) GlueX has begun to explore new territory in previously unknown kinematic regions, taking data of unprecedented statistical quality

∗) Initial production-process studies (SDMEs) go hand in hand with the development and refinement of PWA tools (collaboration with JPAC)

∗) Interesting physics-results:

- Studies of SDMEs,
- First measurement of $a_2(1320)$ cross section,
- Upper limits set for the $\pi_1(1600)$,
- ...

∗) ... and many more things to come!

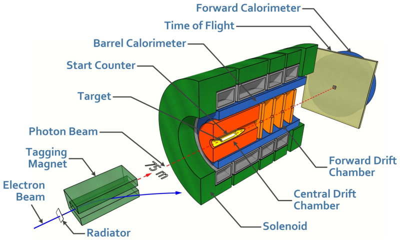

⇒ Exciting treasures to be lifted from upcoming GlueX-II and -III data!

Thank You!

Additional Slides

2-meson photoproduction formalism

Two perspectives on 2-meson photoproduction:

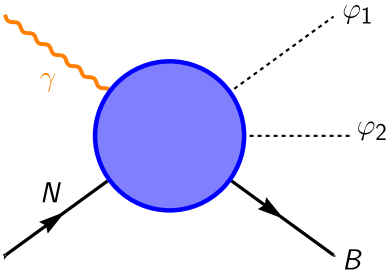

Meson spectroscopy (this talk)

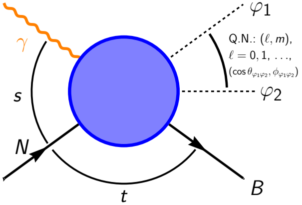

Baryon spectroscopy

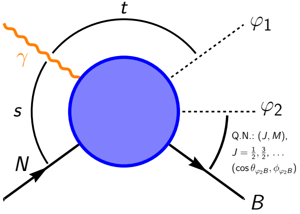

- $\ast$) 5 kin. variables: $\{s, t, m, \Omega = (\theta, \phi)\}$
- $\ast$) 8 helicitiy configurations:
  $\lambda_\gamma = \pm 1, \lambda_1 = \pm\frac{1}{2}, \lambda_2 = \pm\frac{1}{2}.$

Partial-wave expand in helicity-basis, e.g. for 'meson-meson-case':

$$\mathcal{A}_{\lambda_\gamma;\lambda_1\lambda_2}\left(s, t, m^2, \theta, \phi\right) = \sum_{\ell=0,1,\ldots}^{\infty} \sum_{m=-\ell}^{+\ell} \mathcal{T}^{(\ell)}_{\lambda_\gamma, m;\lambda_1\lambda_2}\left(s, t, m^2\right) Y_\ell^m(\theta, \phi)\,.$$

Intensity is the amplitude squared: $I(\Omega) = \sum_{L,M}\left\{H^0(L, M) + \boldsymbol{P}_\gamma \cdot \boldsymbol{H}(L, M)\right\} Y_L^M(\Omega)\,.$

$a_2(1320)$-photoproduction - amplitudes

*) Kinematics: 3 angles $(\cos\theta_\eta, \phi_\eta, \Phi)$ (cf. the above) in rest-frame of decaying resonance (e.g. Gottfried-Jackson frame),

*) Amplitudes are eigenstates of the so-called reflectivity $\epsilon = \pm 1$,

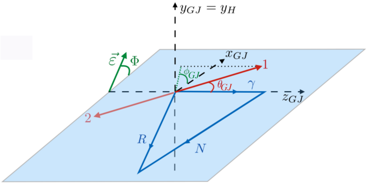

[JPAC, PRD **100**, 5, 054017 (2019)]

*) In high-energy limit: partial-waves with $\epsilon = \pm 1$ are dominated by t-channel exchanges with 'naturality' $\eta = \pm 1$;

Naturality: $\eta := P(-1)^J$, thus:

natural parity $\eta = +1$ for: $J^P = 0^+, 1^-, 2^+, \ldots$

vs.

unnatural parity $\eta = -1$ for: $J^P = 0^-, 1^+, 2^-, \ldots$

*) For $\eta\pi$: positive (negative) reflectivity $\equiv$ natural- (unnatural-) parity exchange,

*) Expand intensity in terms of basis-functions $Z_\ell^m(\Omega, \Phi) := Y_\ell^m(\Omega)\, e^{i\Phi}$:

$$I(\Omega, \Phi, M) = 2\kappa \Big\{ (1 - P_\gamma) \Big[\sum_{\ell, m} [\ell]^{(-)}(M, \vec{x}) \mathrm{Re}\left[Z_\ell^m(\Omega, \Phi) \right] \Big]^2 + (1 - P_\gamma) \Big[\sum_{\ell, m} [\ell]^{(+)}(M, \vec{x}) \mathrm{Im}\left[Z_\ell^m(\Omega, \Phi) \right] \Big]^2$$
$$+ (1 + P_\gamma) \Big[\sum_{\ell, m} [\ell]^{(+)}(M, \vec{x}) \mathrm{Re}\left[Z_\ell^m(\Omega, \Phi) \right] \Big]^2 + (1 + P_\gamma) \Big[\sum_{\ell, m} [\ell]^{(-)}(M, \vec{x}) \mathrm{Im}\left[Z_\ell^m(\Omega, \Phi) \right] \Big]^2 \Big\}.$$